Effect of the temperature on the sintering behavior of CeO2-La2O3 doped with silicate

Caio Daniel Barros de Alecrim
Jorge Luís Marques Garcia
Luiz Francisco dos Santos Neto
Olyverson Lyra Porto
Juliana Pereira Flor
Catia Fredericci

Effect of the temperature on the sintering behavior of CeO_2-La_2O_3 doped with silicate

Caio Daniel Barros de Alecrim[b], Jorge Luís Marques Garcia[a],
Luiz Francisco dos Santos Neto[b], Olyverson Lyra Porto[b],
Juliana Pereira Flor[c] e Catia Fredericci[a*]

a Laboratório de Processos Metalúrgicos, Centro de Tecnologia em Metalurgia e Materiais, Instituto de Pesquisas Tecnológicas do Estado de São Paulo S.A., São Paulo-SP, Brasil.

b Programa de Pós-Graduação do IPT em Processos Industriais

c Fundação de Apoio ao Instituto de Pesquisas Tecnológicas, São Paulo-SP, Brasil.

*E-mail: catiaf@ipt.br

Abstract

This paper evaluates the sintering behavior of CeO_2-La_2O_3-silicate at different temperatures. The sintered compact of this system may be a candidate to be used as a refractory lining for biomass (sugarcane bagasse) gasifier. The raw material (CeO_2-La_2O_3-silicate powder) was characterized by granulometric distribution, differential thermal analysis (DTA), scanning electron microscopy (SEM), energy dispersive spectroscopy (EDS) and dilatometry. Cylindrical compacts of this powder were heat treated at 1200 ºC, 1300 ºC and 1400 ºC for 1 h and characterized by X-ray diffraction (XRD), micro Raman spectroscopy, SEM/EDS, shrinkage and apparent porosity. The results show that the sintering degree of the samples increases with temperature, reaching shrinkage of about 16 % and apparent porosity of 3.5 % at 1400 ºC. The XRD and Raman spectroscopy results revealed that a cerium/lanthanum silicate was formed which is stable against melting at temperature as high as 1400 ºC. The study of the reactivity of the bagasse ash and the CeO_2-La_2O_3-silicate refractory will be presented in a future publication.

Resumo

Este trabalho teve como objetivo avaliar o comportamento de sinterização de CeO_2-La_2O_3-silicato em diferentes temperaturas. O compacto sinterizado desse sistema pode ser um candidato para ser utilizado como um revestimento refratário para gaseificador de biomassa (bagaço-de-cana). A matéria-prima (pó de CeO_2-La_2O_3-silicato) foi analisada por distribuição granulométrica, análise térmica diferencial (DTA), microscopia eletrônica de varredura (MEV), espectroscopia de energia dispersiva (EDS) e dilatometria. Compactos cilíndricos deste pó foram tratados termicamente a 1200 ºC, 1300 ºC and 1400 ºC por 1

h, e caracterizados por difração de raios X (DRX), espectroscopia micro Raman, MEV/EDS, retração e porosidade aparente. Os resultados mostraram que o grau de sinterização das amostras aumentou com a temperatura, atingindo retração em torno de 16 % e porosidade aparente de 3,5 % a 1400 ºC. Os resultados de difração de raios X e espectroscopia Raman indicaram a formação de um silicato de cério-lantânio, que é estável em temperatura tão elevada quanto 1400 ºC. O estudo da reatividade da cinza de bagaço-de-cana e do refratário CeO_2-La_2O_3-silicato será apresentado em publicação futura.

1 Introduction

Brazil is the world's largest producer of sugarcane, with about 641 million tons processed in the 2017/2018 harvest (COMAS, 2018). In several operational units, chemical and biochemical transformations in the processing of sugarcane are carried out at the sugar and alcohol plants. The process starts from the milling generating tons of bagasse which is separated and used for the cogeneration of energy in boilers. When operated at 22 bar and 300 °C to 600 °C, energy self-sufficiency is reached with a tendency for there to be left overs (PERRONE et al., 2010). For the excess of bagasse, an alternative can be developed from the gasification process which is the production of Syngas (CO and H_2), widely used in synthesis in chemical industries or for electricity production with the help of turbines (THEVENIN et al., 2014).

A gasification process can be classified into entrained flow, fluidized bed and moving bed. The entrained flow, for example, operates at an average temperature of 1400 °C and pressure under the range of 20 bar to 70 bar (OMBERG, 2015). According to Bennett et al. (2014), inside reducing-atmosphere gasifiers, reactions between the carbon-based raw material (usually coal, petroleum coke or biomass), water (vapor) and O_2 occur, as follows:

$C + H_2O(g) + O_2$ (shortage) → $CO + H_2 + CO_2$ + residual gases + by-product (ash) + heat
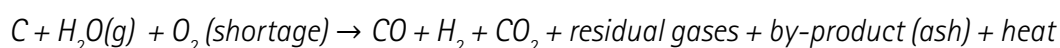
Ashes contain compounds with Si, O, Al, Ca, K, P, Mg, Fe and Ti (FREDERICCI et al., 2014), coming from the macro- and micronutrients of the sugarcane. An important point of the gas synthesis production unit is the knowledge of the generation of ash that can melt at elevated temperatures (~ 1400 ºC). Gasifier walls are covered with refractory materials which must be corrosion resistant against the produced ashes. One of the challenges in the biomass gasifier design is the choice of refractory lining (THEVENIN et al., 2014). According to world levels, most gasifiers are designed for the gasification of coal, petroleum coke and wood chips which present chemical compositions different from the ashes generated by the combustion of sugarcane bagasse (FREDERICCI et al., 2014). Therefore, the reactivity of the ashes, generated by the burning of these biomasses, with refractory materials, optimized for the gasification of coal and coke, may be very different from those known until now, being indispensable studies in this area. Fredericci et al. (2015, 2016, 2017) showed that Al_2O_3, ZrO_2, Cr_2O_3-Al_2O_3-ZrO_2 refractories were reactive with sugarcane bagasse ashes. In addition, Fe^{3+} reduction to metallic iron occurs in a reducing atmosphere.

Ceria (CeO_2) has been shown to be a promising ceramic for the coating of black liquor biomass gasifiers (CHADDOCK, 2006) and a corrosion protection agent in silica refractories in glass melting furnaces (KOBAYASHI, 2002). Kobayashi et al. (2002) reported that silica-based refractories, used in the production of glass (rich in SiO_2, Na_2O and CaO), form silicates at elevated temperatures during glass processing. This is because alkali metal oxide vapors penetrate the pores of the refractory material and react with silica to form low melting silicates, resulting in a high corrosion rate and a loss of mass of the refractory. The authors suggested using of corrosion protectors such as CeO_2, La_2O_3 as well as high-melting-point calcium-aluminum silicates in the silica refractories. In conclusion, they reported that the presence of cerium oxide reduces the corrosion by alkali metals. Chaddock (2006) studied ceria-based refractories for black liquor gasification (rich alkali metal compounds) and reported that CeO_2 is chemically resistant to this waste.

The motivation for the present work was first to study the sintering behavior of the ceria-lantania-silicate system to produce a refractory material. Secondly, in a future work, to study its reactivity with ash of sugarcane bagasse at an elevated temperature (1400 ^{o}C). To our best knowledge, this is the first time that the CeO_2-La_2O_3-silicate system is studied to be used in laboratory tests as a material for coating a biomass (sugarcane bagasse) gasifier.

2 Experimental procedure

2.1 Raw material

Policer powder, from ENGECER, was used. According to the manufacturer, it is composed of CeO_2, La_2O_3, silicate and of an organic deflocculant. The kind of silicate presented in the formulation was not reported because it is an industrial protected product. Thus, only a scanning electron microscopy analysis was performed to determine its morphology and its chemical elements.

2.2 Characterization of the raw material

CeO_2 was characterized by scanning electron microscopy (SEM), JEOL model JSM 6300 used in the mode of secondary electrons, with a voltage of 20 kV. The powder was placed and compacted on a carbon tape and covered with a thin layer of gold deposited under vacuum. Differential thermal analysis (DTA) was carried out using a NETZSCH model 409S equipment, with alumina crucible, under an ambient atmosphere (air), with a heating rate of 8 °C/min, from the ambient temperature up to 1400 °C.

The particle size distribution was determined using the Particle Insight equipment, with sodium hexametaphosphate as the deflocculant.

2.3 Compaction and Sintering

Cylindrical specimens with a diameter of about 20 mm (2.00 g of powder) were uniaxially pressed at 62.5 MPa. The specimens had sufficient mechanical resistance to be handled and placed on an alumina ceramic plate.

A rectangular specimen (12.92 x 2.95 x 6.19) mm³ was also prepared using a pressure of 62.5 MPa for analysis using a Netzsch dilatometer, model DIL 402, for determining the sintering temperatures. A heating rate of 8 ºC/min and a spring compressive force of 0.2 N were used. From the result of this test, temperatures of heat treatments were determined as well as the dwell time of 1 h. As the sintering furnace (Maitec – FE-1700) presents exposed resistances of molybdenum disilicide, an alumina shield was placed in the furnace chamber to prevent overheating of the edges of the specimens relative to their center. The furnace was heated at 8 ºC/min up to 800 ºC, at 5 ºC/min from 800 ºC to 1200 ºC and finaly at 3 ºC/min from 1200 ºC to 1400 ºC. The heat treated samples were cooled in the furnace by natural convection.

2.4 Characterization of sintered specimens

The apparent porosity (PA) of the specimens was measured by the Archimedes method, using the **Equation 1***:*

$$PA = \frac{mu - ms}{mu - mi} \; x100 \qquad\qquad \textbf{(Equation \; 1)}$$

The dry mass (ms) was measured after drying the specimens for 24 h at 100 ºC. The immersed mass (mi) was determined after immersion in distilled water for 24 h and the humid one was measured after removing the surface excess water (MONTORO et al., 2011). Five specimens obtained from different temperatures (1200 ºC to 1400 ºC) were analyzed and the data were presented as mean value and as standard deviation.

Fractured specimens were covered with a thin layer of gold and palladium for microstructural analyses, using a Quanta 3D FEG microscope coupled to an EDAX system of energy dispersive spectroscopy (EDS). The microstructural analyses were carried out under a voltage of 20 kV in the mode of secondary electrons.

One of the specimens, treated at 1400 ºC for 1 h, was milled and sieved in a 325 mesh screen for X-ray diffraction analyses in a XRD 6000 diffractometer, using Cu Kα radiation, with a scanning of 1°/min and a range of 5° to 60° (2θ).

To complement the X-ray diffraction analyses, Raman spectroscopy was used. The Raman spectra were obtained from the surface of the sample without polishing, using a Confocal Raman spectrophotometer (Witec model alpha 500R - GmbH, Germany), containing a double monochromator, a diffraction grating of 600 lines/mm and a CCD detector. The focusing of the

laser on the sample and the collection of the scattered radiation at 180° were done through a Witec metallurgical microscope and objective lens of 100X CF Plan with aperture number of 0.55. An excitation line in the visible region was used at 532 nm of an Argon laser (Witec brand, S/N 100-1665-154). Each spectrum corresponds to the average of 100 accumulations acquired with integration time of 50 s.

3 Results and discussion

3.1 Distribution of particle size of the raw material and EDS elementary analysis

Figure 1 shows the granulometric distribution curve of the powder used in this work. Observing the results in **Figure 1** (volume %), it is noted that the maximum particle size is approximately 26.5 μm,

Figure 1 – Particle size distribution analysis of the Policer powder (CeO$_2$–La$_2$O$_3$–silicate)
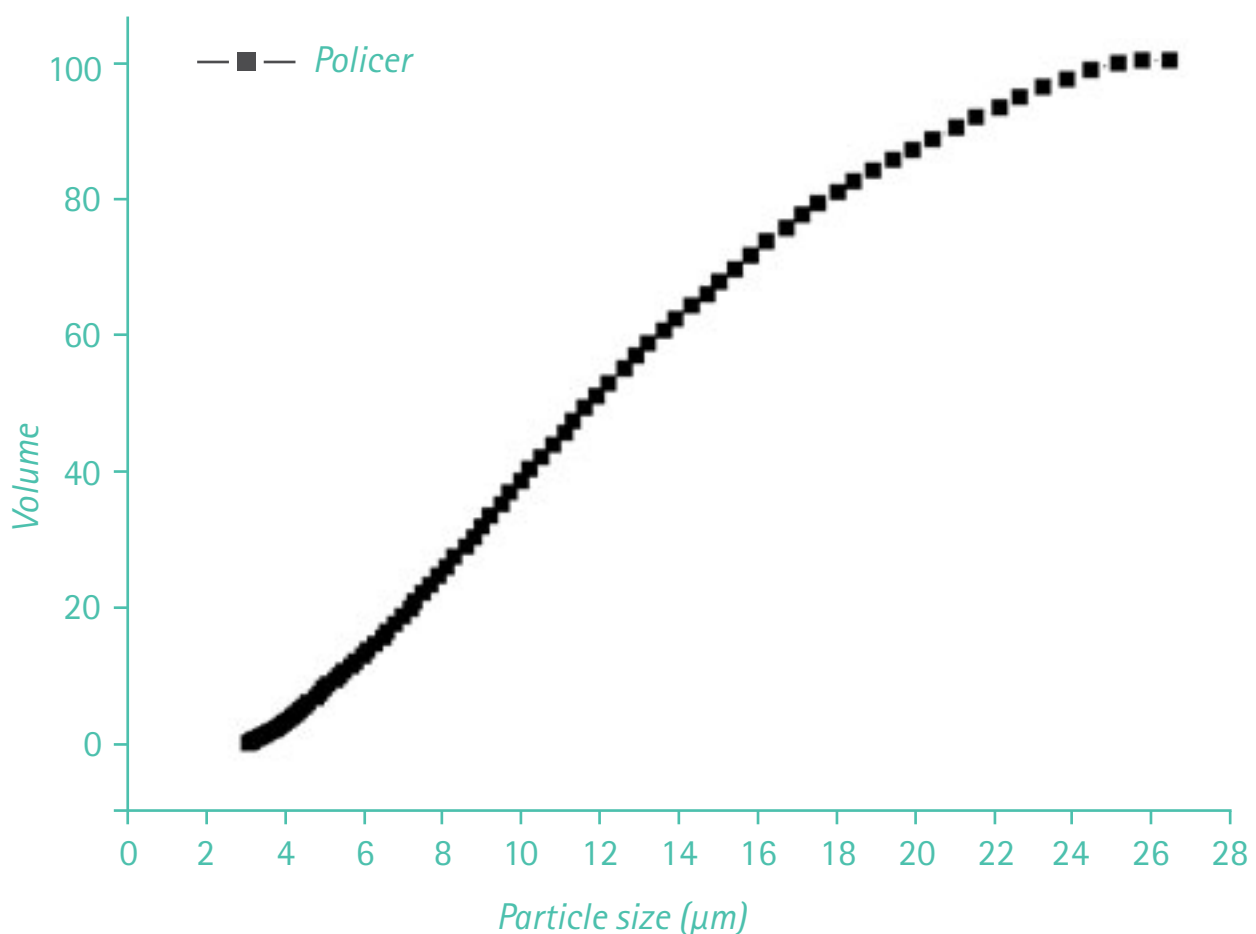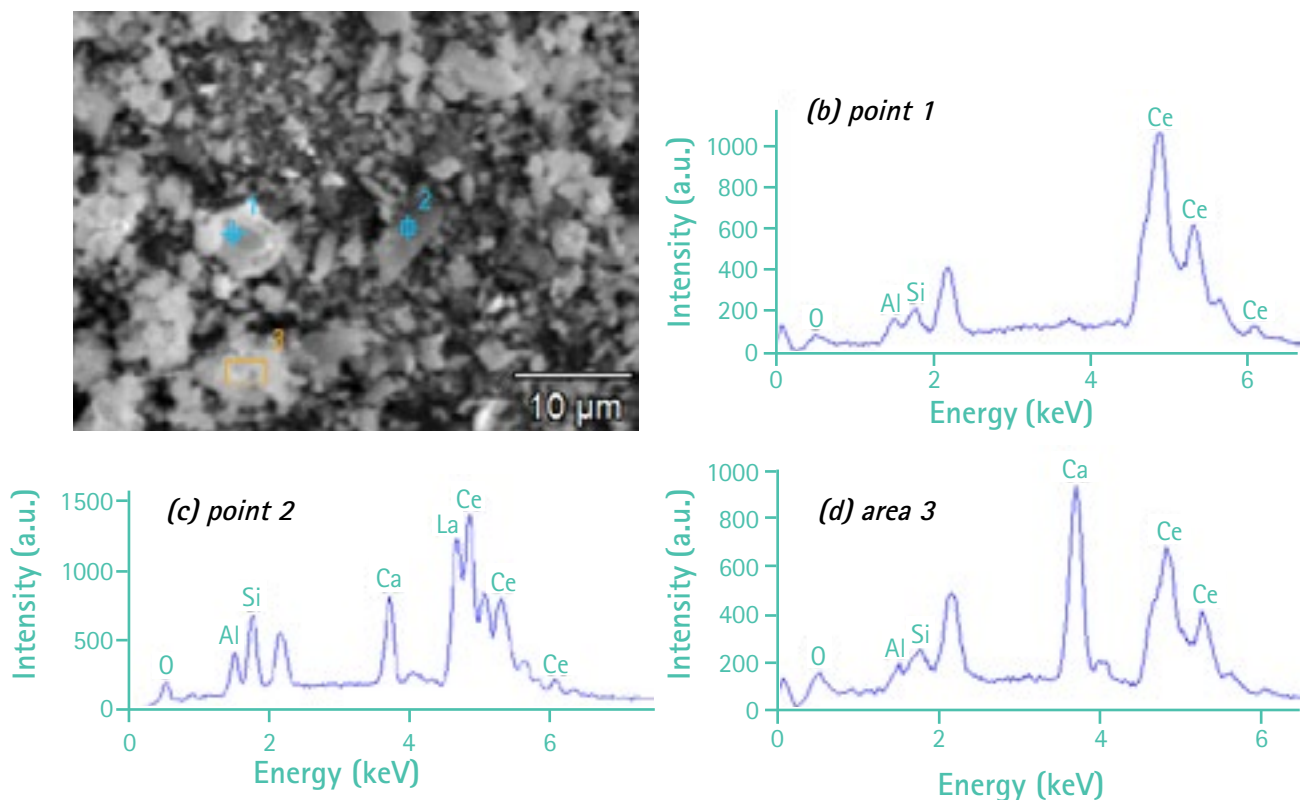

Source: created by authors

the minimum measured size is 3 μm, limited by the measuring range of the equipment, and the mean size (50 vol%) is approximately 12 μm, with a unimodal distribution. Therefore, the powder has a granulometry with particle size smaller than 325 mesh (below 40 μm) which was easily compacted.

__Figure 2__ shows the scanning electron micrograph of the powder used along with EDS analyses at two points and one area. It is possible to observe that the powder contains the elements O, Al, Si, Ca, La, Ce and Fe, indicating that it is a mixture of rare earth oxides with a calcium iron aluminum silicate. Rare earths have similar properties and, in a separation process, oxide mixtures are generally obtained (LIANG et al., 2011). Therefore, this system shows what Kobayashi et al. (2002) identified as possible corrosion protectors for refractories in contact with silica, alkali and earth alkali metal oxides melted at elevated temperatures.

Figure 2 – (a) Micrographs obtained by SEM, in the secondary electron mode, of the Policer powder, (b), (c) and (d) EDS spectra of points 1 and 2 and area 3,respectively, shown in micrograph (a)
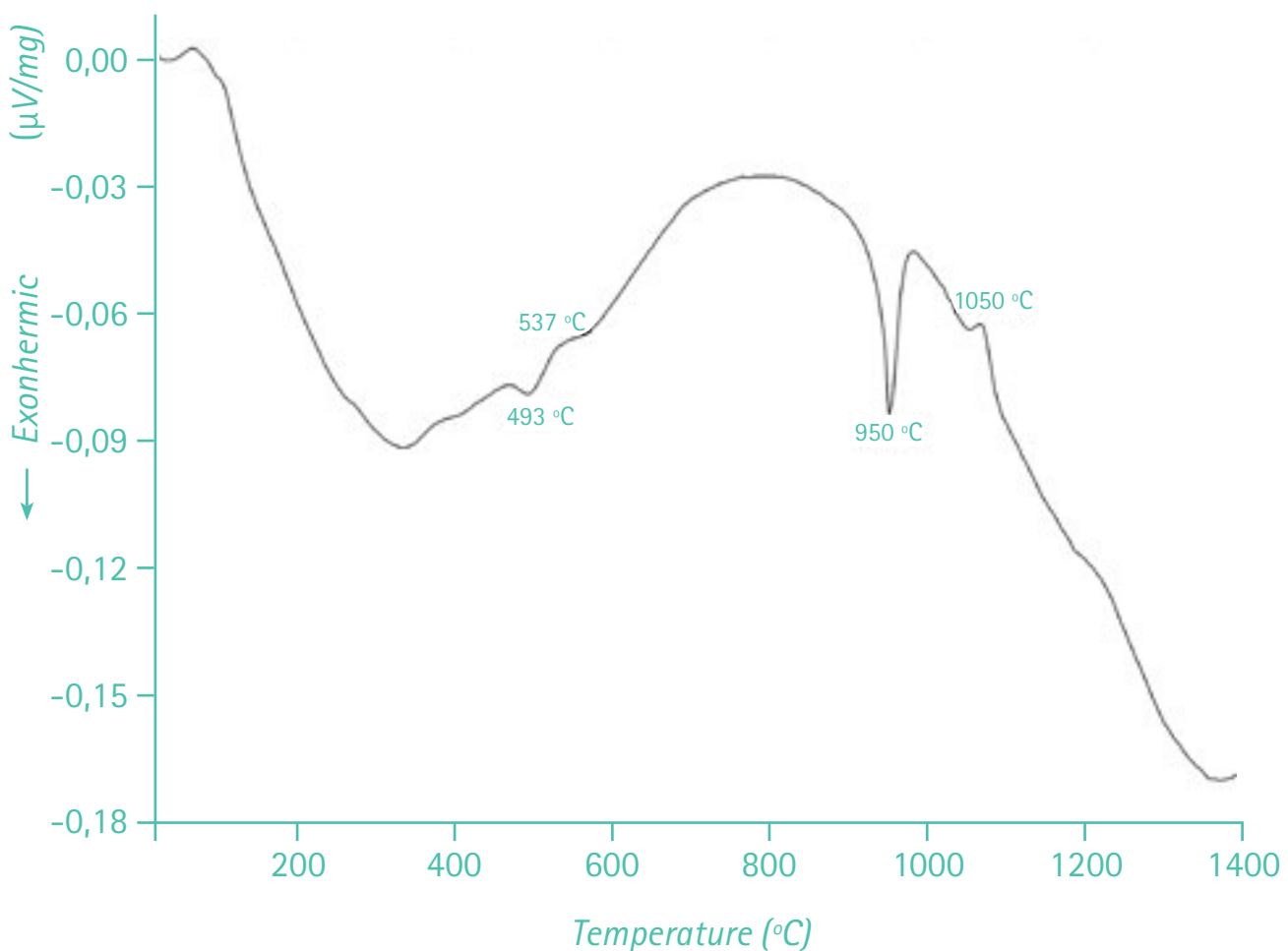

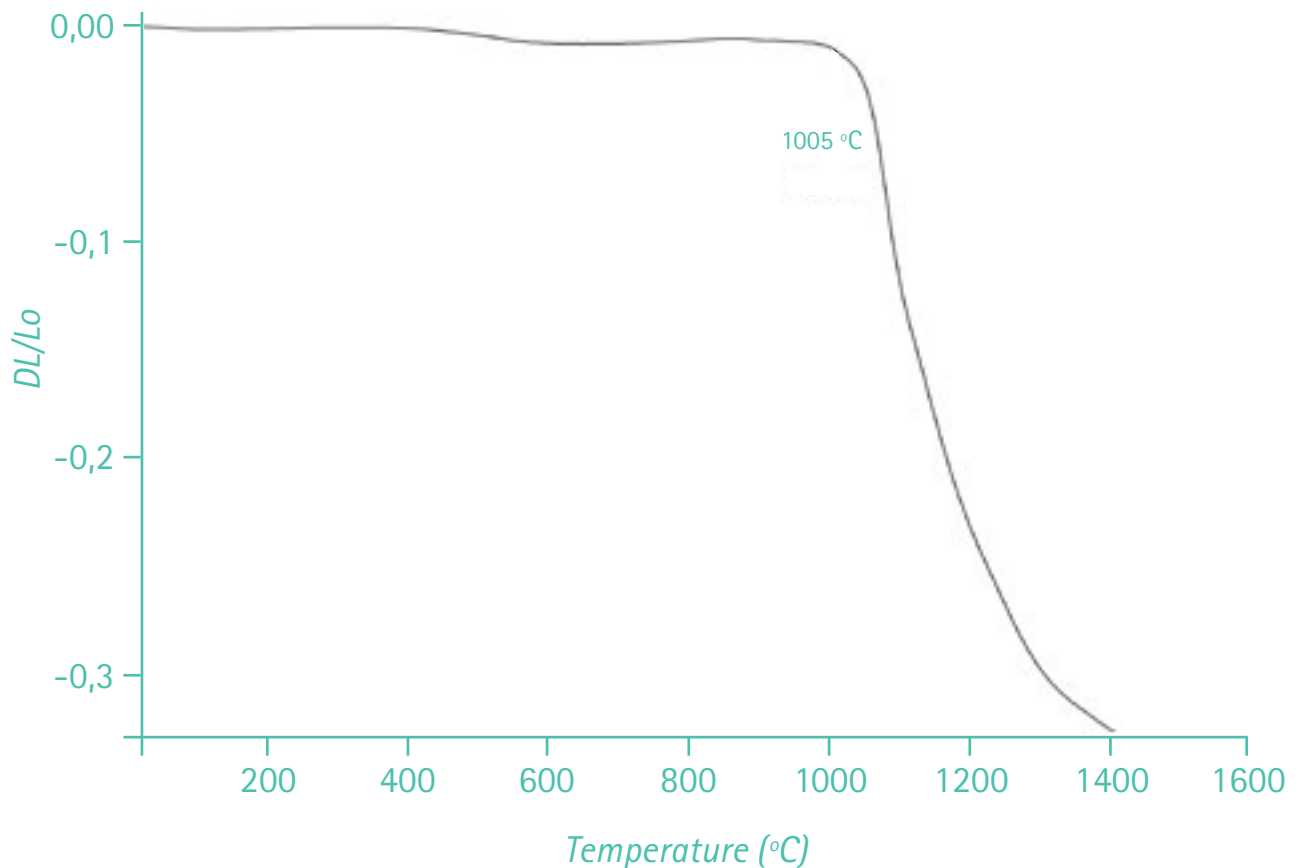*__Source:__ created by authors*

3.2 DTA and Dilatometric analyzes

Figure 3 shows the differential thermal analysis curve of the Policer powder. There are two discrete bands between 493 °C and 565 °C that can be attributed to the burning of the organic deflocculant; one sharp band at 950 °C and another discrete band at 1050 °C, both exothermic, which shows the possibility of a reaction between the silicate and CeO_2/La_2O_3. No endothermic bands related to melting of the crystalline phase were observed which is a positive result indicating that the sintered material do not forms liquid phase in temperature as high as 1400 °C. It is interesting to observe in the dilatometric analysis (*Figure 4*) that the sample begins to have a significant degree of shrinkage after 1005 °C indicating the beginning of the sintering process for this system. There is a tendency for sintering stabilization at around 1400 °C, since the curve tends to be stable above this temperature. From this result, temperatures such as 1200 °C, 1300 °C and 1400 °C were chosen for the sintering study.

Figure 3 – Thermal analysis curve of Policer powder (CeO$_2$/La$_2$O$_3$/Silicate)

Source: created by authors

Figure 4 – Dilatometric curve of the Policer powder (CeO$_2$/La$_2$O$_3$/Silicate)


Source: created by authors

3.3 Scanning electron microscopy of the sintered specimens

In **Figure 5**, it is possible to observe that in the specimens treated at 1200 °C for 1 h, the grains are in the initial phase of sintering (neck formation), the porosity is high, the grains are small (< 5 µm), some are round, while others are in the form of rods. The micrograph of the specimen treated at 1300 °C for 1 h (**Figure 5b**) shows a greater number of rod-shaped crystals, but it still has considerable porosity. **Figure 5c** shows a micrograph of the specimen treated at 1400 °C for 1 h. It is possible to observe the increase in the size of rounded grains and those with rod morphology, all larger than those presented in the previous figures (**5a and 5b**), as expected. The increase in the temperature increases the atomic diffusion and the grain growth. The dilatometric analysis indicates that shrinkage is approximately maximum at 1400 °C (**Figure 4**). The analysis of dispersive energy spectroscopy (**Figure 6b and 6c**) shows the compositions referring to the morphologies presented in the sintered specimens. The rounded grains are rich in Ce (87.04 % by weight), corresponding to CeO$_2$ grains with small amounts of Ca, Si and Al. The rods are rich in La (42.59 %), Ce (30.91 %) and Si (12.14 %) indicating to be a silicate.
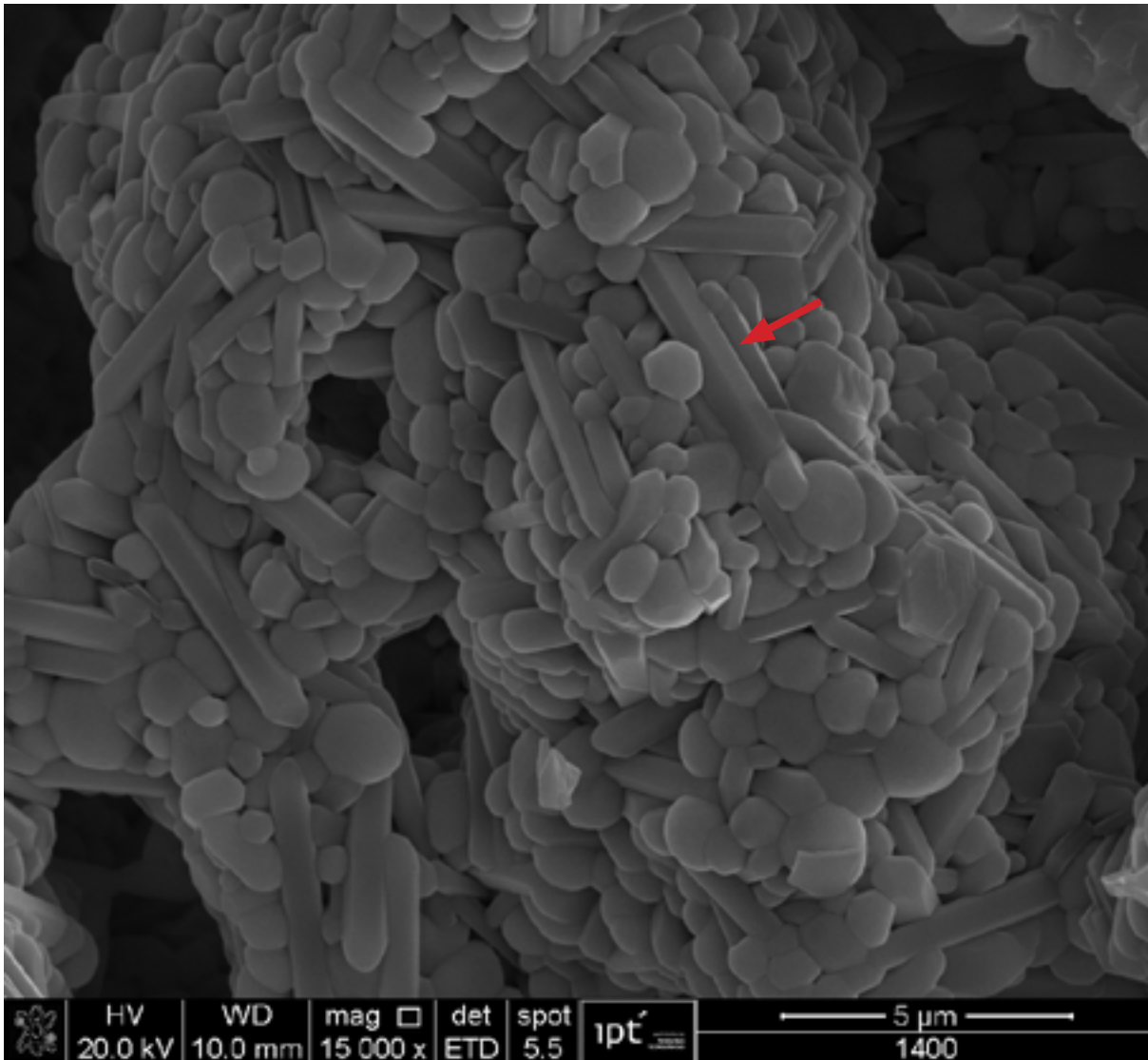
Figure 5 – (a), (b) and (c) micrographs obtained by scanning electron microscopy, in the secondary electron mode, of fracture surfaces of samples treated at 1200 ºC, 1300 ºC and 1400 ºC for 1 h. The green arrows indicate the formation of necks and grain boundaries between the particles and, the red ones, the formation of crystals in the form of rods
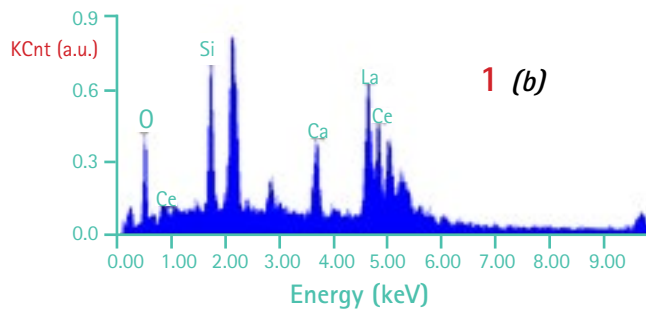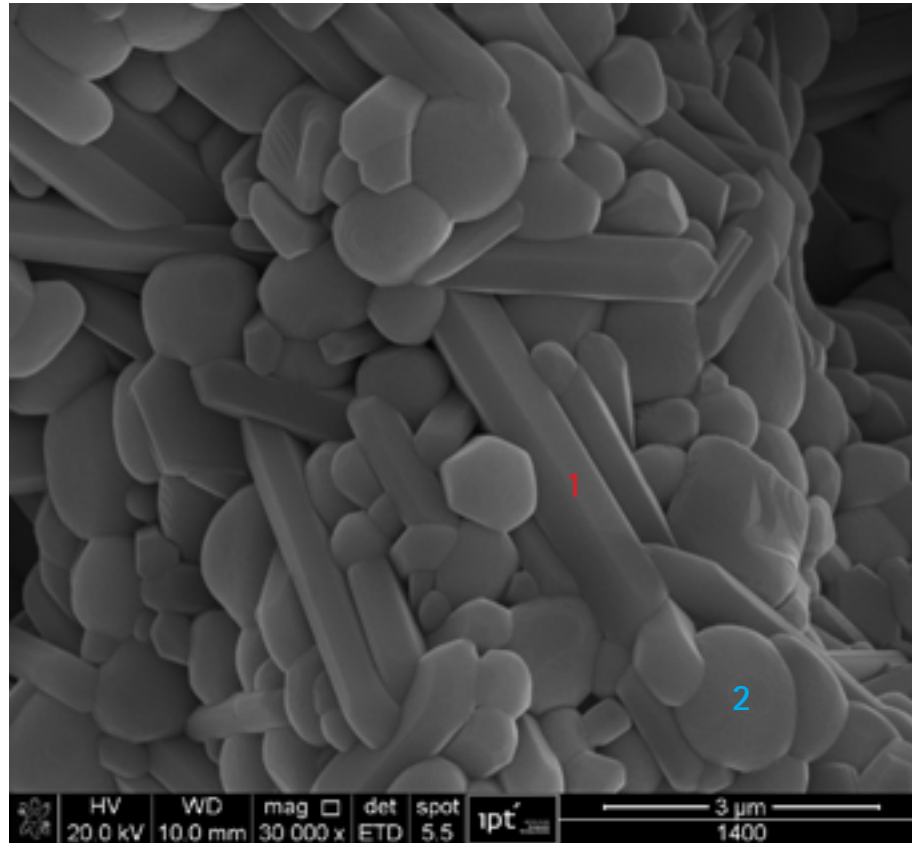

(a) 1200 ºC

(b) 1300 ºC
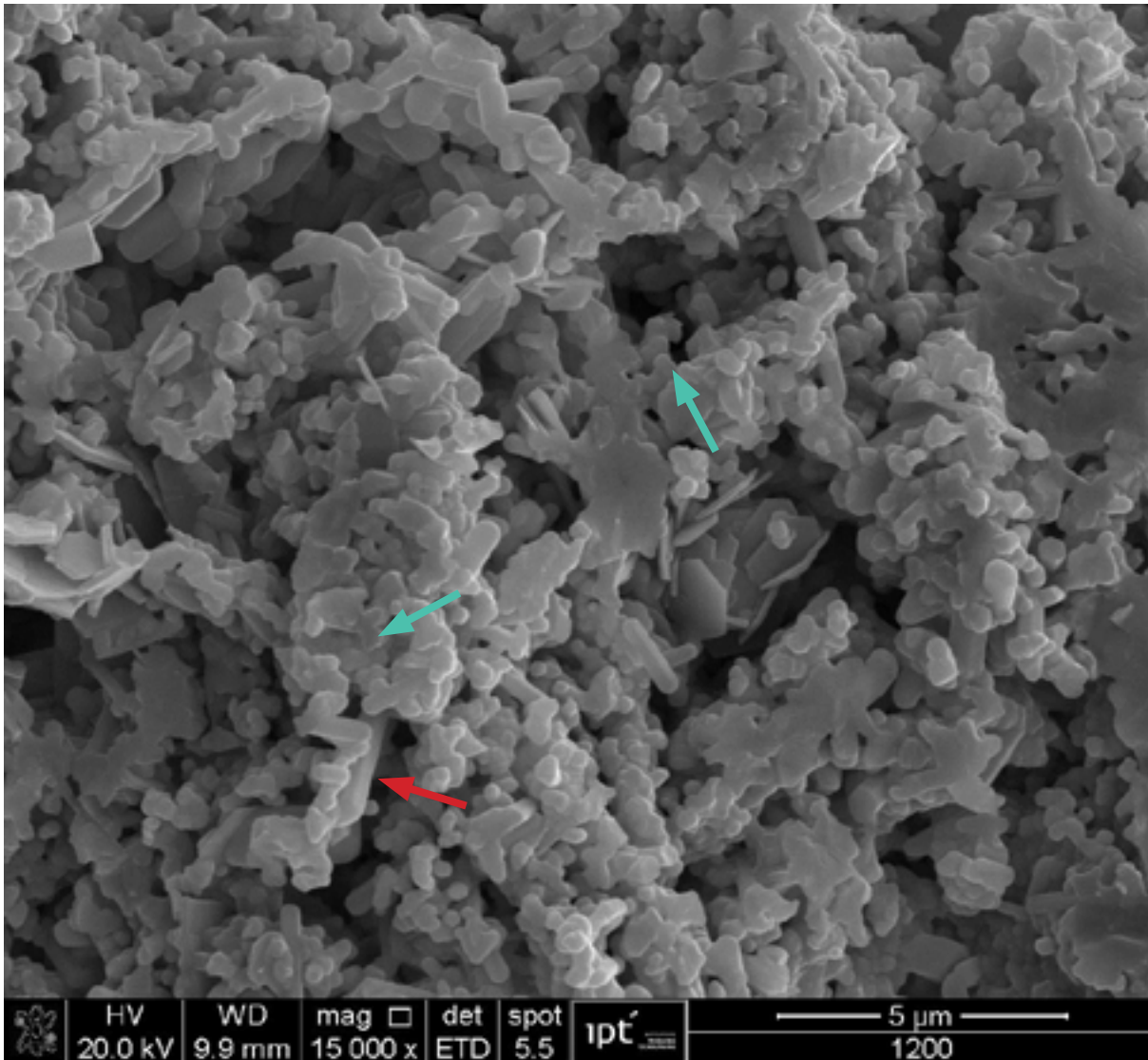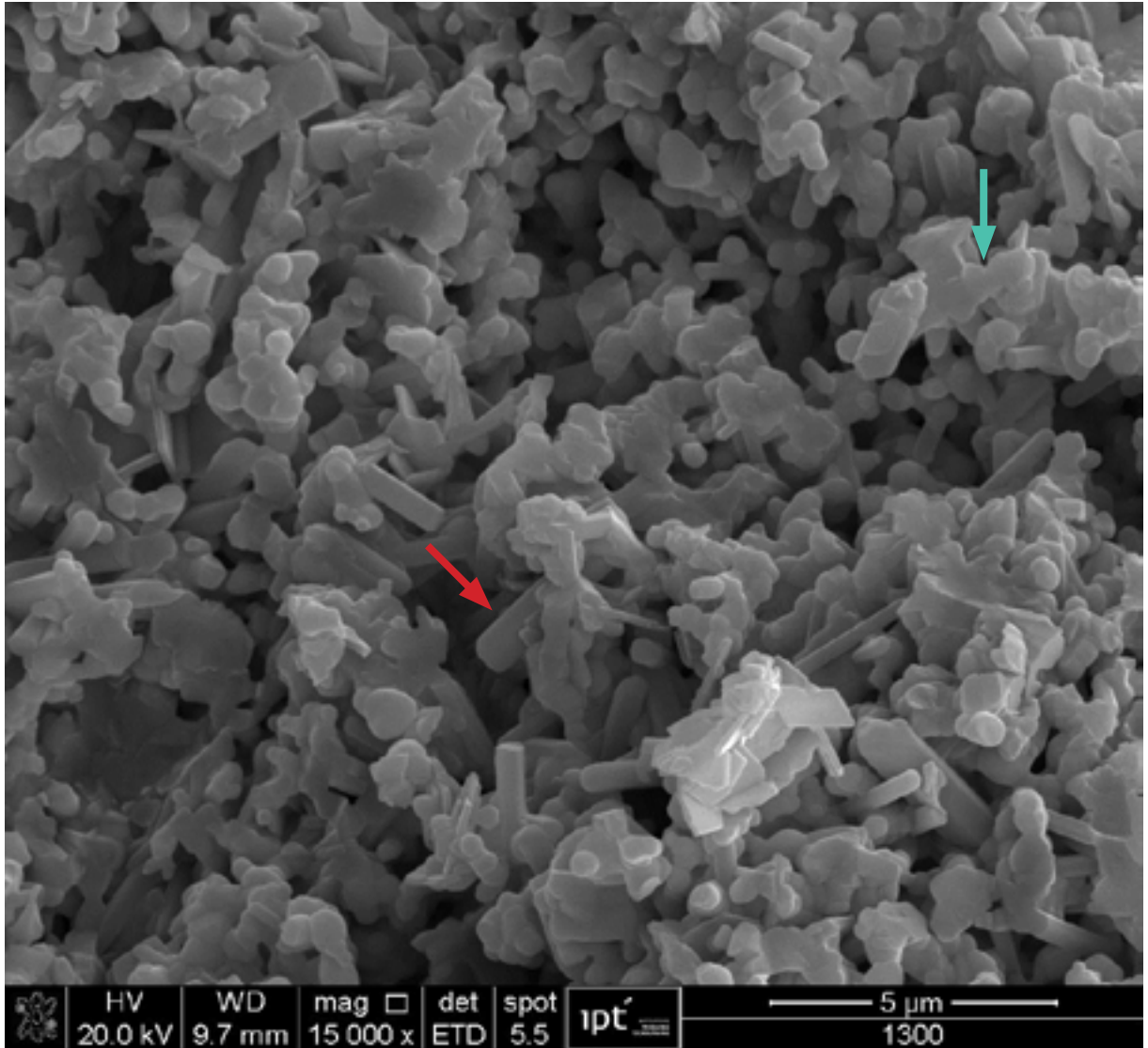
(c) 1400 ºC

Figure 6 – (a) micrographs obtained by scanning electron microscopy, in the secondary electron mode of samples treated at 1400 ºC for 1 h, (b) and (c) EDS spectra and elemental chemical composition of points 1 and 2 shown in figure a. Au e Pd are from the recovering for the analysis

Element	Wt %	At %
OK	08.74	33.18
SiK	12.14	26.27
CaK	05.62	08.52
LaL	42.59	18.62
CeL	30.91	13.40
Matrix	Correction	ZAF
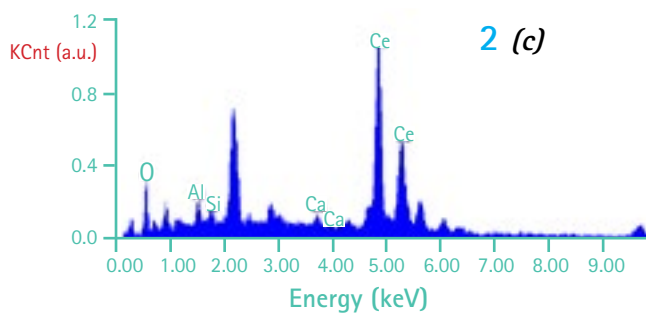
| Element	Wt %	At %
OK	06.84	33.93
ALK	03.33	09.79
SiK	01.68	04.74
CaK	01.12	02.21
CeL	87.04	49.32
Matrix	Correction	ZAF

Source: created by authors

3.4 X-Ray diffraction and Raman spectroscopy

Figure 7 shows the X-ray diffraction pattern of the sample treated at 1400 ℃ for 1 h. The diffractogram indicates peaks relative to cerium oxide (JCPDS-00-034-0394) and peaks relative to a cerium silicate ($Ce_{4.667}$ (SiO_4)$_3$O-JCPDS 00-043-0441), but with a little dislocation of 2θ in relation to this phase. Hutchison (2015) reported that little literature exists on a La/Ce-silicate phase.

A double silicate of cerium and lanthanum was not found in the standard database (PDF-4) of X-ray diffraction. Thus, the lanthanum must be present in the structure of the silicate as a substituent atom. Weimmerskirch et al. (2015) studied the effect of heat treatment of silicon doped ceria thin films and observed the formation of $Ce_{4.667}$ (SiO_4)$_3$O. Kepinski et al. (2005) reported SiO_2 and $La(NO_3)_2$ reaction as a function of temperature and they verified that it leads to the formation of lanthanum silicate due to the ability of lanthanum to break Si-O-Si bonds. These authors studied Raman spectra of the thermally treated samples and reported the presence of intense bands at 844 cm^{-1} to 859 cm^{-1}, referring it to the individual tetrahedra of [SiO_4]. *Figure 8* shows the Raman spectra of a sample treated at 1400 ℃ for 1 h, obtained in this work. Several spectra were performed in different regions of the sample, but, in *Figure 8*, only the spectra of two different regions (a and b) are presented which correspond to the only two patterns found in the analyses in various regions of the sample. The band at 460 cm^{-1} corresponds to the CeO_2 standard (REDDY et al., 2005) and the band at 854 cm^{-1} confirms the presence of silicate with individual tetrahedral units, corroborating the results found in X-ray diffraction and SEM.

Figure 7 – X-ray diffraction of the sample treated at 1400 ℃ for 1 h
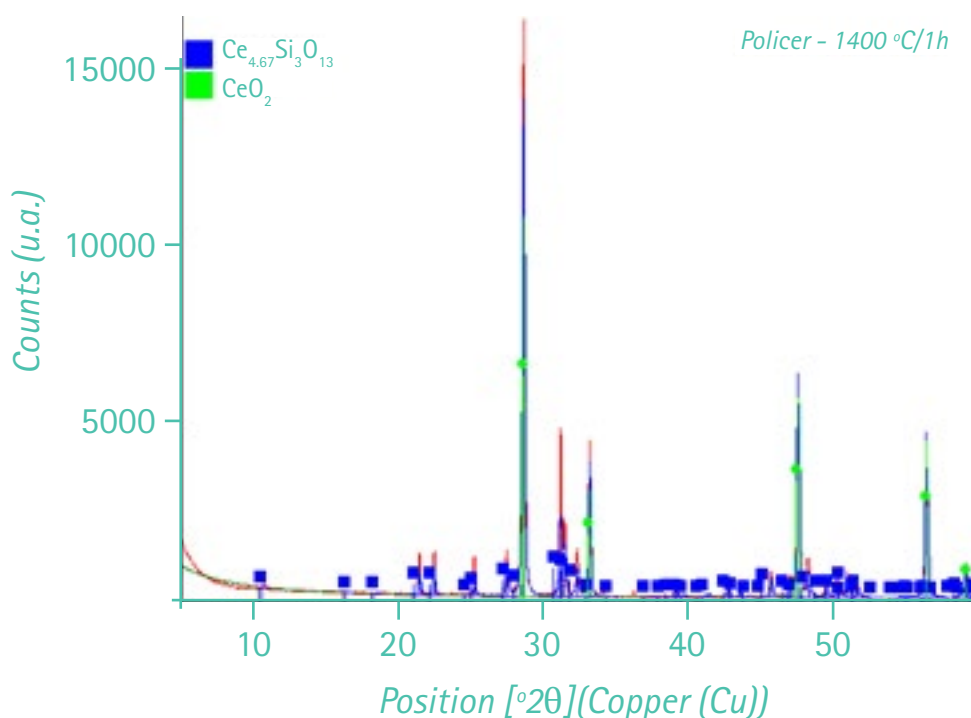
Source: created by authors

*Figure 8 – Raman spectra of the specimen treated at 1400 ºC for 1 h*
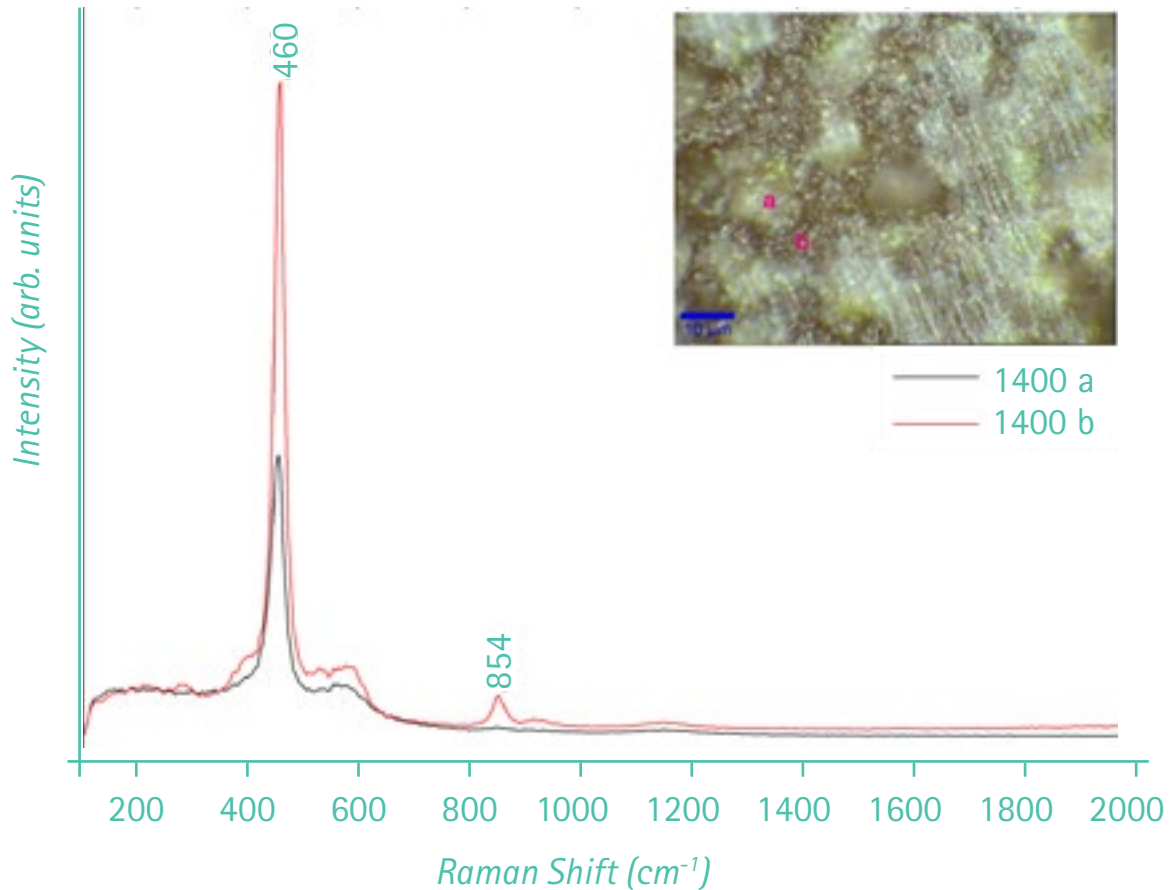
Source: created by authors

3.5 Shrinkage

Figure 9 *shows the shrinkage and the apparent porosity of the samples as a function of the temperature. It can be seen that, for 1200 °C, 1300 °C and 1400 °C , there was a sample size decrease of approximately 1.8 %, 4.1 % and 16.5 %, respectively, indicating that the densification occurs between 1300 ºC and 1400 ºC. The behavior of the apparent porosity is inverse to that of the shrinkage, indicating that the larger the contraction the smaller the apparent porosity.*

The results indicate that the sample treated at 1400 ºC for 1 h formed cerium lanthanum silicate of a low apparent porosity (3.5 %) which may be of interest for reactivity tests with sugarcane bagasse ashes. The results of the reactivity study will be published in the future.

Figure 9 – Shrinkage analysis of specimens with uniaxial pressure of 62.5 MPa as a function of temperature.
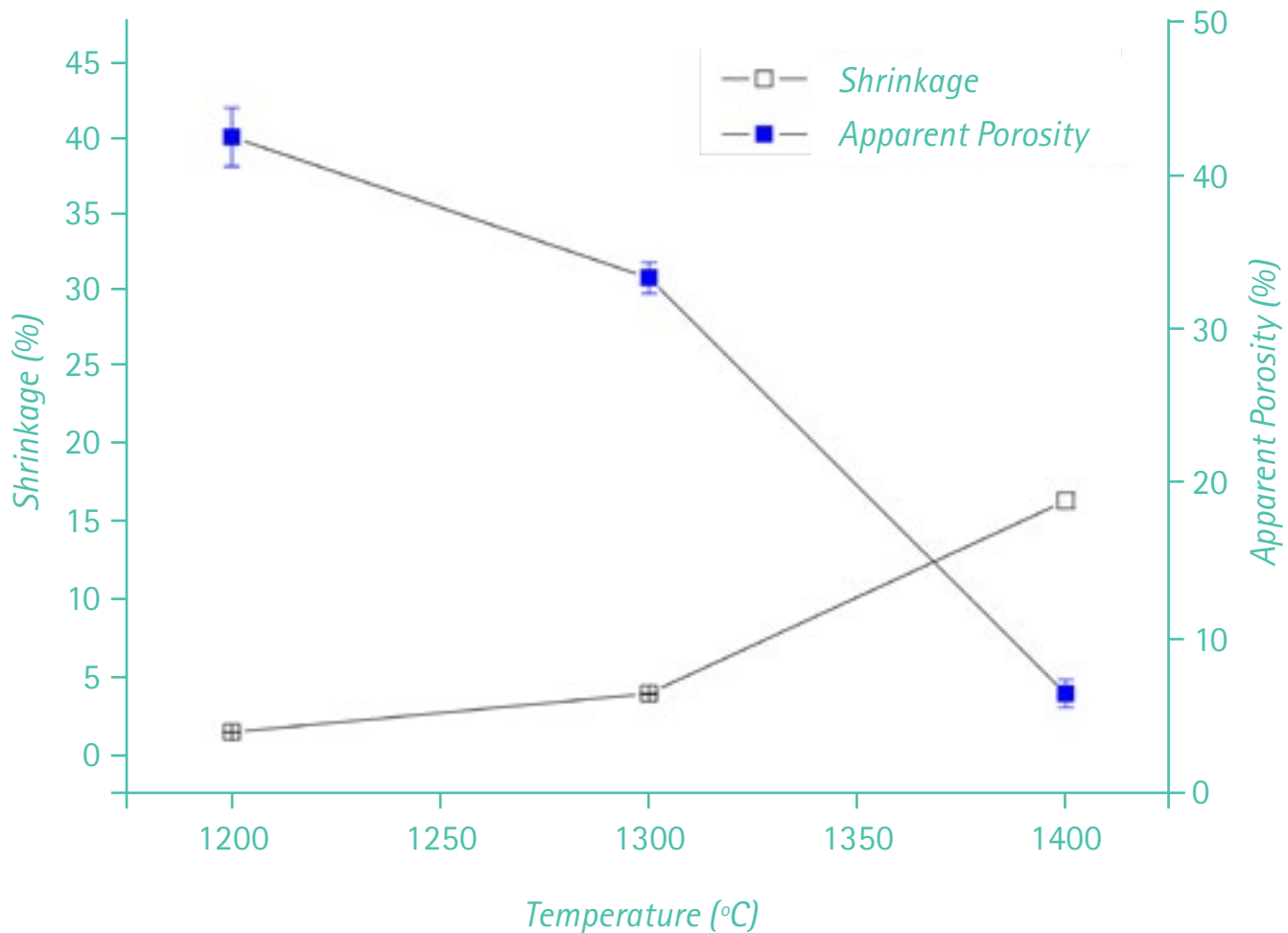
4 Conclusions

In this study, the effect of the temperature on the sintering of CeO_2-La_2O_3-Silicate powder was investigated. The results of dilatometry showed that the sintering of this powder begins at temperatures higher than 1005 °C and reaches approximately the maximum shrinkage at 1400 °C. X-ray diffraction in conjunction with Raman spectroscopy and EDS analyses indicated the formation of a cerium-lanthanum silicate with rod-like morphology determined by scanning electron microscopy. This silicate phase did not melt at temperatures up to 1400 °C.

5 Acknowledgment

6 References

BENNETT, J. P.; KWONG, K-S. Failure mechanism in high chrome oxide gasifier refractories. **Metallurgical and Materials Transactions** A, v. 42A, n. 4, p. 888-904, Apr. 2011.

CHADDOCK, J. **Refractory for Black Liquor Gasifiers**. Washington, DC: US Department of Energy, 2006. p. 1. (Energy Efficiency and Renewable Energy – Biomass Program).

COMAS, C. C. Brasil é o maior produtor mundial de cana-de-açúcar. **Neo Mundo**, June, 21 2018. Available in:. <http://www.neomondo.org.br/2018/06/21/brasil-e-o-maior-produtor-mundial-de-cana-de-acucar/>. Accessed in: Nov. 4 2018.

FREDERICCI, C.; CRUZ, I. A.; RIBEIRO, T. R.; FUKUHARA, T. Y. Corrosão de refratário à base de Al2O3 por cinza de cana de açúcar em atmosfera redutora. In: CONGRESSO BRASILEIRO DE CERÂMICA, 60., 2016, Águas de Lindóia. **Anais...** São Paulo: Associação Brasileira de Cerâmica, 2016. p. 1-12.

FREDERICCI, C.; ETT, G.; SILVA, G. F. B. L.; FERREIRA NETO, J. B.; LANDGRAF, F. J. G.; INDELICATO, R. L.; RIBEIRO, T. R. An analysis of Brazilian sugarcane bagasse ash behavior under thermal gasification. **Chemical and Biological Technologies in Agriculture**, p. 1-15, Dec. 2014.

FREDERICCI, C.; MENOSSI, M.S.; CRUZ, I.A.; INDELICATO, R.L. - Corrosão de refratários à base de Cr2O3 e Al2O3 por cinza de cana de açúcar. In: CONGRESSO BRASILEIRO DE CERÂMICA, 59, 2015, Barra do Coqueiros. **Anais...** São Paulo: Associação Brasileira de Cerâmica, 2015. p. 1-12.

FREDERICCI, C.; RIBEIRO, T. R. Corrosão de refratários à base de ZrO2 por cinza de cana-de-açúcar em atmosfera redutora. In: CONGRESSO BRASILEIRO DE CERÂMICA, 61., 2017, Gramado. **Anais...** São Paulo: Associação Brasileira de Cerâmica, 2017. p. 1-12

HUTCHISON, C. A. **Microstructure and corrosion intermediate level wasteforms fabricated using novel thermal techniques**. 2017. 223 f. Thesis – Department of Materials, Imperial College London, London, 2017.

KEPINSKI, L.; MISTA, W.; OKAL, J.; DROZD, M.; MACZKA, M. Interfacial reactions and silicate formation in high surface SiO2 impregnated with La nitrate. **Solid State Sciences**, v. 7, p. 1300–1311, 2005.

KOBAYASHI, W. T.; DA SILVA, E. L.; PASKOCIMAS, C.A. **US Patent 6,455,102 B1**: Method for producing corrosion prevention. 2002. p. 1-9.

LIANG, S.; BROITMAN, E.; WANG, Y.; CAO, A.; VESER, G. Highly stable, mesoporous mixed lanthanum–cerium oxides with tailored structure and reducibility. **Journal of Materials Science**, v. 46, p. 2928-2937, 2011.

MONTORO, S. R.; SHIINO, M. Y.; CRUZ, T. G; CIOFFI, M. O. A.; WOORWALD, H. J. C. Influence of voids oh the flexural resistance of the NCF/RTM6 composite. **Procedia Engineering**, v. 10, p. 3220-3225, 2011.

OMBERG, O. S. **Techno–economical evaluation of suitable conversion technology for the production of biofuels from wood biomass**. 2015. 116 f. Thesis - Faculty of Environmental Science and Technology, Norwegian University of Life Sciences, Akershus, 2015.

PERRONE, C.C.; APPEL, L.G.; MAIA LELLIS, G.L.; FERREIRA, F.M.; DE SOUSA, A.M.; FERREIRA-LEITÃO,V.S. Ethanol: an evaluation of its scientific and technological development and network of players during the period of 1995 to 2009. **Waste Biomass Valor**, v. 2, n. 1, p. 17-32, Feb. 2010.

REDDY, B.M.; KHAN, A.; LAKSHMANAN, P. Structural Characterization of Nanosized CeO2-SiO2, CeO2-TiO2, and CeO2-ZrO2 Catalysts by XRD, Raman, and HREM Techniques. **Journal of Physical Chemistry B**, v. 109, p. 3355-3363, 2005.

THEVENIN, G.; POIRIER J.; PRIGENT P.; FOURCAULT A.; J. P. ROBERT-ARNOUIL J. P.; EDME E.; MARIAS F.; DEMARTHON R. Modelling and design of a refractory lining for a biomass gasification reactor fed by a plasma torch. **Waste and Biomass Valorization**, v. 5, n. 5, p. 865-877, Oct. 2014.

WEIMMERSKIRCH-AUBATIN, J.; STOFFEL, M.; BOUCHÉ, A.; VERGNAT, M.; RINNERT, H. Optical properties of Ce-doped SiO2 films: From isolated Ce3+ ions to formation of cerium silicate. **Journal of Alloys and Compounds**, v. 622, p. 358–361, Feb. 2015.